Jet Structure Studies in Small Systems [†]

Zoltán Varga [1,2,*] [ID]**, Róbert Vértesi** [1] [ID] **and Gergely Gábor Barnaföldi** [1] [ID]

[1]   Wigner Research Centre for Physics, P.O. Box 49, H-1525 Budapest, Hungary;
      vertesi.robert@wigner.mta.hu (R.V.); barnafoldi.gergely@wigner.mta.hu (G.G.B.)
[2]   Department of Theoretical Physics, Institute of Physics, Faculty of Science, Eötvös Loránd University,
      Pázmány Péter sétány 1/A, H-1117 Budapest, Hungary
[*]   Correspondence: varga.zoltan@wigner.mta.hu
[†]   This paper is based on the talk at the 18th Zimányi School, Budapest, Hungary, 3–7 December 2018.

Abstract: A study investigating a possible jet shape dependence on the charged event multiplicity was performed on collision samples generated by Monte–Carlo (MC) event generators PYTHIA and HIJING++. We calculated the integral jet shape and found a significant modification caused by multiple-parton interactions. By interchanging and enabling different model ingredients in the simulations and analyzing the results in several p_T bins and event multiplicity classes, we found a characteristic jet size measure that was independent of the chosen tunes, settings, and jet reconstruction algorithms.

Keywords: jet physics; jet structure; jet shapes; color reconnection; multiple-parton interactions; high-energy collisions

PACS: 13.87.-a; 25.75.-q; 25.75.Ag; 25.75.Dw

1. Introduction

The discovery of collective-like behavior in high-multiplicity proton-proton (pp) and proton-nucleus (pA) collisions was one of the major surprises in early LHC results [1,2]. The collective-like behavior previously found in large systems, manifested in long-range correlations and a sizeable azimuthal anisotropy, have traditionally been considered as a signature proving the presence of the quark-gluon plasma (QGP). The creation of the QGP in high-energy nucleus-nucleus (AA) collisions can also be investigated by studying the structure of jets and their modification that leads to the well-known jet quenching phenomenon [3,4]. Whether QGP is created in small systems like pp collisions is still an open question [5]. However, the presence of the QGP is not necessary to explaining collectivity: Relatively soft vacuum-QCD effects such as multiple-parton interactions (MPI) and color reconnection (CR) can also produce a similar behavior [6,7]. These interactions, at least in principle, can modify the jet shapes in even small systems. Although experimental confirmation is not yet available, a recent phenomenology study also suggests the modification of hard processes by soft vacuum-QCD effects in a high-multiplicity environment [8].

MPI is also expected to depend on flavor [9]. Fragmentation of heavy-flavor jets is expected to differ from light-flavor jets because of color charge and mass effects. The internal structures of heavy-flavor jets may therefore provide a deeper insight into the flavor-dependent development of jets and their connection to the underlying event (UE). This paper continues our previous studies [10,11] aimed at the evolution of jet structure patterns and their dependence on simulation components.

2. Analysis

We used PYTHIA 8.226 and HIJING++ Monte–Carlo (MC) generators to simulate pp collision events at $\sqrt{s} = 7$ TeV [12,13]. Three different PYTHIA tunes were investigated, the Monash 2013 tune with the NNPDF2.3LO PDF set [14,15], the Monash* tune with NNPDF2.3LO [16], and tune 4C with the CTEQ6L1 PDF set [17,18]. Collisions with and without multiple-parton interactions and color reconnection were simulated and compared to each other [10,11]. We only considered particles above the transverse momentum threshold $p_T^{track} > 0.15$ GeV/c. We carried out a full jet reconstruction using the anti-k_T, k_T, and Cambridge–Aachen jet reconstruction algorithms, which are part of the FASTJET software package [19]. These choices are typical in jet shape analyses [20]. The multiplicity-integrated jet shape studies of CMS were used as a benchmark for our current multiplicity-differential studies [10,20]. Therefore we chose the jet resolution parameter as $R = 0.7$ and applied a fiducial cut so that the jets were contained in the CMS acceptance $|\eta| < 1$. We did not apply underlying event subtraction in the jet cones. We investigated the jets within the 15 GeV/c $< p_T^{jet} < 400$ GeV/c transverse momentum range, where multiplicity-differential studies on real data are feasible in the near future.

We chose the following two jet shape measures to study the multiplicity-dependent behavior of the jet structure: The Ψ integral jet shape (or momentum fraction) and the ρ differential jet shape (or momentum density fraction) [21,22]. The former one gives the average fraction of the jet transverse momentum contained inside a sub-cone of radius r around the jet axis, the latter one is the momentum profile of the jet, i.e., the average transverse momentum of the particles contained inside an annulus with a δr width and boundaries r_a and r_b. The exact formulae are given by:

$$\Psi(r) = \frac{1}{p_T^{jet}} \sum_{r_i < r} p_T^i \quad \text{and} \quad \rho(r) = \frac{1}{\delta r} \frac{1}{p_T^{jet}} \sum_{r_a < r_i < r_b} p_T^i \tag{1}$$

respectively, where p_T^i is the transverse momentum of the selected particle and p_T^{jet} is the transverse momentum of the jet. The distance r_i of the given particle from the jet axis is calculated as $r_i = \sqrt{(\phi_i - \phi_{jet})^2 + (\eta_i - \eta_{jet})^2}$, where ϕ is the azimuthal angle and η is the pseudorapidity. For a better understanding, we noted that the aforementioned observables are connected with the equations:

$$\Psi(r) = \int_0^r \rho(r')dr', \quad \text{and} \quad \Psi(R) = \int_0^R \rho(r')dr' = 1, \tag{2}$$

where R is the jet resolution parameter. The differential and integral jet shapes were calculated for the above mentioned p_T^{jet} range. The three tunes reproduced the CMS results within statistical errors [10,11].

3. Results

The multiplicity distributions (multiplicity is defined as the number of charged final state particles in a given collision event) were very similar for the three tunes used in our simulations, as shown in the left panel of Figure 1. However, a significant change is observed when we do not consider the effects of the color reconnection and/or the multiple-parton interactions. Without the CR, the multiplicity distribution becomes wider. If we also switch off the MPI, the multiplicity distribution becomes much narrower compared to the setting where both of them are applied. The width of the multiplicity distribution, however, is not sensitive to the choice of the CR model. In the right panel of Figure 1, we plot the mean values of the multiplicity distributions in events where we reconstructed a jet of a given transverse momentum. We did not exclude non-leading jets in our analysis, but we also investigate the effects of selecting only leading jets later in this paper. As expected, the average event multiplicity grew with the transverse momentum of the selected jet.
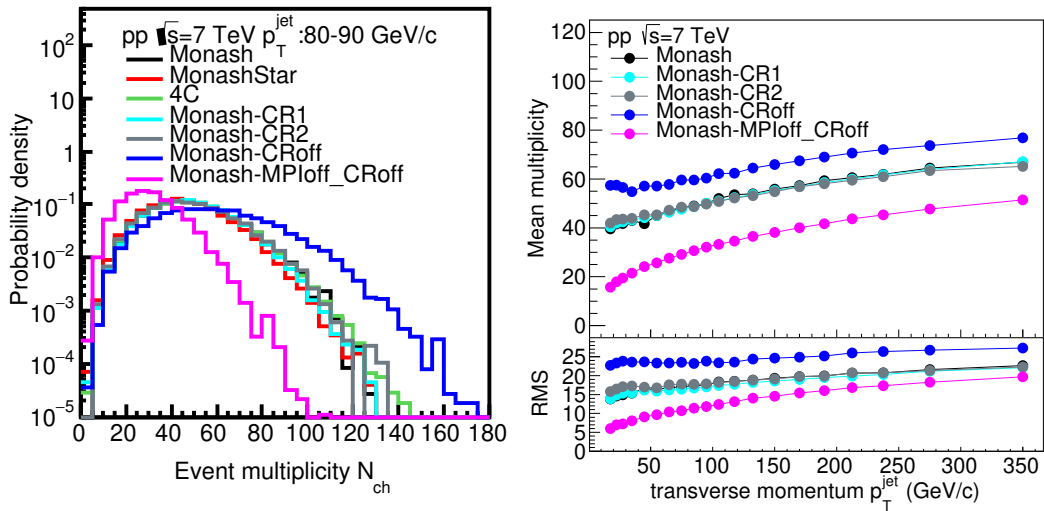
Figure 1. (**Left**) Multiplicity distributions for different tunes and settings in events where the p_T^{jet} of the reconstructed jets falls in a given p_T bin; (**Right**) The mean values of the distributions are shown as a function of the p_T^{jet}. The RMS is the relative mean squared value of the distribution.

The integral jet shape with $r = 0.2$ is shown in Figure 2 to compare the effects of the different tunes and settings. As expected [23], we see similar trends for the multiplicity distributions of the tunes. However, there is a substantial difference between the different MPI and CR settings. The most significant difference in the jet shapes was caused by turning off the MPI, which further supports the current view that the MPI contributions need to be included to correctly describe the jet shapes. We note that we did not subtract the underlying event from the jet. Further investigation is necessary to understand whether the interplay between the UE and the observed hard process is significantly modified by the MPI.
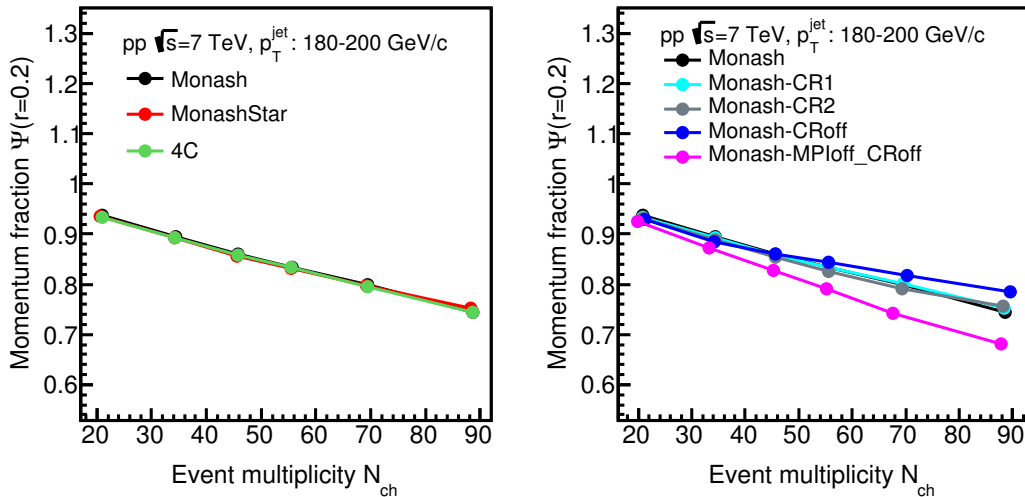

Figure 2. (**Left**) Integrated jet shape for different tunes; (**Right**) Integrated jet shape for different settings.

In order to gain a more comprehensive picture, we use the current differential jet shape to investigate the multiplicity dependence of the jet shapes. On the left side of Figure 3, we categorize the events into a high and low multiplicity class. The differential jet shapes of both categories are compared to the multiplicity-integrated momentum density (ρ_{MI}), computed without any selection in multiplicity. A multiplicity dependence is observed. The jets in the higher multiplicity bin appear to be wider while the jets in the lower multiplicity bin appear to be narrower. This is a trivial multiplicity dependence

since the event multiplicity strongly correlates with the jet multiplicity. In our previous work, we canceled this trivial multiplicity dependence by applying a double ratio across the different tunes [10].

In the right panel of Figure 3, we plotted the $\rho(r)/\rho_{MI}$ ratio for the low- and high-multiplicty bins divided by the ρ_{MI} curve. In this way, the difference compared to the ρ_{MI} (black) curve is more visible. We also observed that the $\rho(r)/\rho_{MI}$ curves obtained from the low- and high-multiplicty classes intersect each other at a particular radius inside the jet cone.

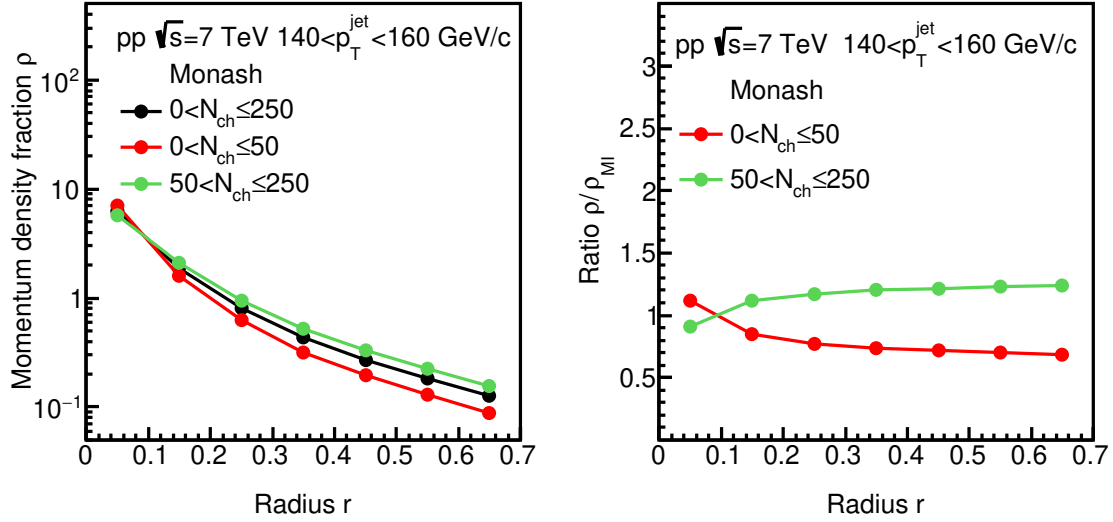**Figure 3.** (**Left**) Differential jet shape for low- and high-multiplicity bins; (**Right**) The differential jet shape ρ divided by the ρ_{MI} to emphasize the difference.

We also investigated whether the choice of multiplicity bins affects the location of the intersection point by categorizing the events into several smaller event multiplicity bins. We found that all the ρ/ρ_{MI} curves corresponding to these different multiplicity classes intersect each other at approximately the same radius, as can be seen on the left panel of Figure 4. Therefore we named this specific r value R_{fix}. The R_{fix} depends, however, on the transverse momentum of the jet, as shown in the right panel of Figure 4. The $R_{fix}(p_T^{jet})$ curve goes in a fashion expected by a Lorentz boost and converges to a constant value at higher energies [10].

Since we use a linear interpolation between the points of ρ/ρ_{MI}, the value of R_{fix} will have a slight dependence on the bin width in r (δr), especially at higher p_T values where the value of R_{fix} is smaller. To make sure that the results are robust enough, we repeated the analysis with narrower bins ($\delta r = 0.05$). In the left panel of Figure 5, we show ρ with this finer r binning, while in the right panel of the same figure we plotted the p_T^{jet} dependence of R_{fix}. We can see that the effects by the choice of bin width is rather small and does not change the conclusions, so we do not have to sacrifice the current statistics for finer binnings.

Using different settings in PYTHIA changes the physics enough to expect different jet structures after jet reconstruction. All of the k_T, Cambridge–Aachen and anti-k_T jet clustering algorithms that we investigated reconstructed the jet structures differently since they had different susceptibility to the underlying event. We therefore investigated the effects of varying the physics settings and used three different jet reconstruction algorithms (Figure 6). We conclude that the presence of R_{fix} was very robust for the different physics selections, as its stability was neither an artifact of the particular choice of jet reconstruction algorithms, nor did it depend strongly on the underlying event. We note that R_{fix} is localized to lower r values, therefore we do not expect significant influence from effects that are mostly visible at higher r values, such as the modification of the UE or higher order corrections to the parton shower [24,25].
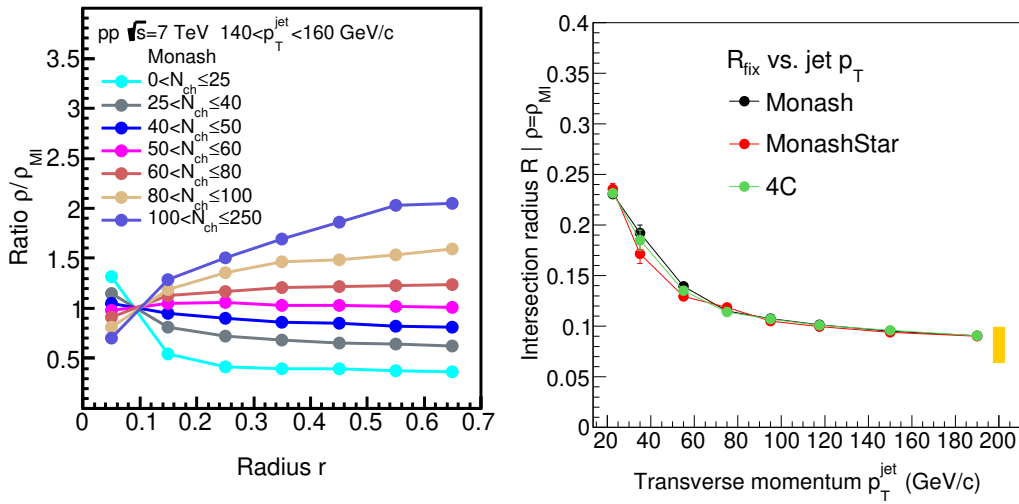
Figure 4. (**Left**) Ratio $\rho/\rho_{\rm MI}$ of the differential jet structure over the multiplicity-integrated curve for many different multiplicity bins; (**Right**) The $p_{\rm T}^{\rm jet}$ dependence of $R_{\rm fix}$ with $\delta r = 0.1$. The systematic uncertainty from the choice of δr is shown as the yellow band.
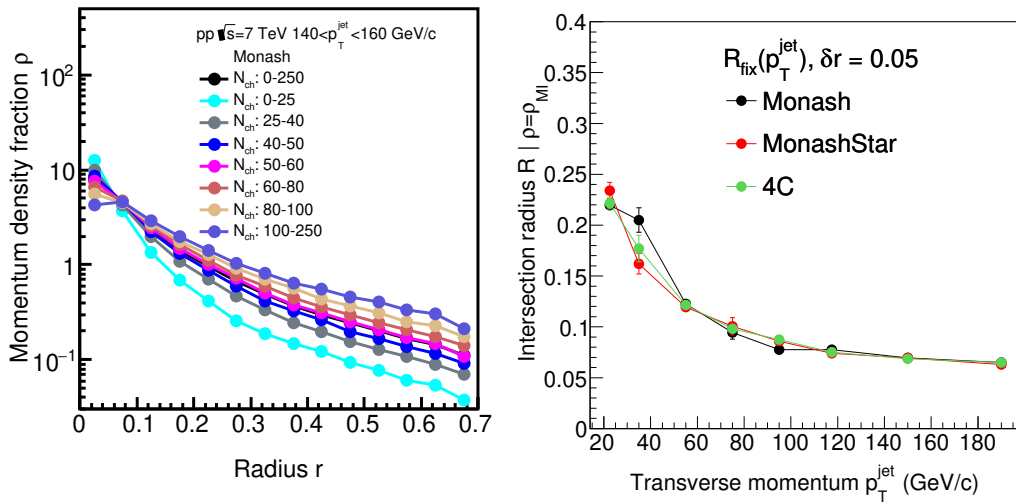

Figure 5. (**Left**) The differential jet shape for many different multiplicity bins with finer ($\delta r = 0.05$) binnings; (**Right**) The $p_{\rm T}^{\rm jet}$ dependence of $R_{\rm fix}$ with finer ($\delta r = 0.05$) binnings.
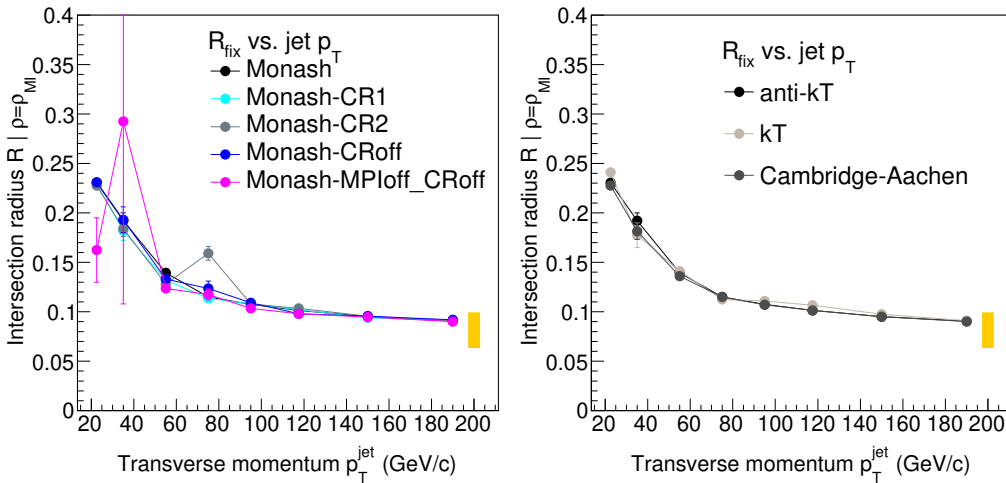

Figure 6. The evolution of $R_{\rm fix}$ with the $p_{\rm T}^{\rm jet}$ for different settings (**left**); and for different jet reconstruction algorithms (**right**).

We also computed the differential jet shapes using a different MC generator. We selected HIJING++ for this purpose because it implements a mechanism of creating the underlying event and QCD effects on the soft-hard boundary that is different from PYTHIA. HIJING++ uses the PYTHIA jet fragmentation, therefore we do not expect any difference during the later stages. Instead of MPI as implemented in PYTHIA, HIJING++ uses minijet production. Differences at lower momenta may arise below the minijet cutoff. In case of the p_T and multiplicity distributions, these effects do not exceed the variation caused by applying different tunes in PYTHIA.

In the case of HIJING++, we used two different PDF sets. The results show quantitatively the same R_{fix} dependence on p_T^{jet} within systematic errors, as can be seen in the left panel of Figure 7. Jets originating from different flavors undergo different fragmentation due to both the color-charge effect and the dead-cone effect [26]. We compared flavor-inclusive jets to heavy-flavor (beauty and charm) jets in the right panel of Figure 7. We ensured that heavy flavor comes from the initial stages by only enabling leading order processes in PYTHIA. We compared these to leading and subleading flavor-inclusive jets.

It should be noted that the effect of non-leading jets is negligible on the R_{fix}. Although the overall tendency of heavy-flavor R_{fix} is similar to that observed for light flavor, there is also a clear quantitative difference between heavy and light flavors, which points to a different jet structure. The leading b jets differ for higher p_T^{jet} and the leading c jets for lower p_T^{jet}. This suggests that the interplay between the mass and color-charge effects is non-trivial and needs further investigation. One possibility for that would be a parallel study of the UE and the fragmentation region corresponding to a heavy-flavor trigger, in a similar manner to [27]. From all the above, we can assume that R_{fix} is a property of the jets that is associated with the final state.

We also repeated the same analysis by selecting only the leading and sub-leading jets. We observed no significant difference compared to the case where all the jets were used (right panel of Figure 7).
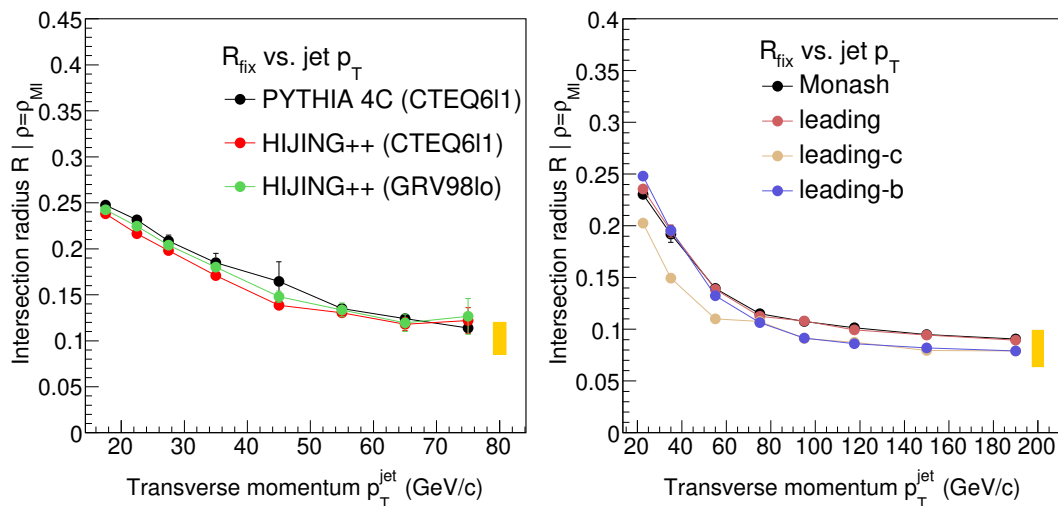

Figure 7. (**Left**) The p_T^{jet} dependence of R_{fix} for the PYTHIA 4C tune is compared with HIJING++; (**Right**) Comparison of different jet selections for the PYTHIA Monash tune.

4. Conclusions

We conducted a systematic study on jet structures for pp collisions using MC generators PYTHIA and HIJING++. We investigated the effects of CR and MPI on jet shapes and showed that not considering the effects of CR and MPI causes significant jet shape modification. We introduced a characteristic jet size (R_{fix}) that depends only on the p_T of the jets but is independent of the jet reconstruction algorithms, MC generators, parton density functions, and even the choice of simulation parameters such as CR and MPI [10,11]. We have also shown that the choice of δr does not change our

conclusions about R_{fix}. These observations suggest that R_{fix} is an inherent property of the jets and is characteristic to the space-time evolution of the parton shower at a given momentum.

However, R_{fix} does depend on the flavor of the jet. Flavor-dependent jet structure studies may be a way to access mass versus color charge effects that is complimentary to hadron- or jet-production cross-section measurements. We believe that our findings motivate further phenomenology studies as well as cross-checks with real data to gain a deeper understanding on flavor-dependent jet fragmentation. Another direction for future research could be to investigate the effects of MPI on jets without the underlying event. This could be done either by choosing an observable that depends very weakly on the underlying event [9], or by the parallel understanding of the underlying event and the fragmentation region [27].

References

1.　Yan, L.; Ollitrault, J.Y. Universal fluctuation-driven eccentricities in proton-proton, proton-nucleus and nucleus-nucleus collisions. *Phys. Rev. Lett.* **2014**, *112*, 082301. [CrossRef]

2.　Khachatryan, V.; Sirunyan, A.M.; Tumasyan, A.; Adam, W.; Bergauer, T.; Dragicevic, M.; Erö, J.; Fabjan, C.; Friedl, M.; Frühwirth, R.; et al. Observation of Long-Range Near-Side Angular Correlations in Proton-Proton Collisions at the LHC. *J. High Energy Phys.* **2010**, *2010*, 091. [CrossRef]

3.　Adcox, K.; Adler, S.S.; Ajitanand, N.N.; Akiba, Y.; Alexander, J.; Aphecetche, L.; Arai, Y.; Aronson, S.H.; Averbeck, R.; Awes, T.C.; et al. Supression of hadrons with large transverse momentum in central Au+Au collisions at $\sqrt{s_{NN}}$ = 130 GeV. *Phys. Rev. Lett.* **2001**, *88*, 022301. [CrossRef] [PubMed]

4.　Gyulassy, M.; Levai, P.; Vitev, I. Jet Quenching in Thin Quark-Gluon Plasmas I: Formalism. *Nucl. Phys. B* **2000**, *571*, 197–233. [CrossRef]

5.　Dusling, K.; Li, W.; Schenke, B. Novel collective phenomena in high-energy proton–proton and proton–nucleus collisions. *Int. J. Mod. Phys. E* **2016**, *25*, 1630002. [CrossRef]

6.　Ortiz, A.; Bencédi, G.; Bello, H. Revealing the source of the radial flow patterns in proton–proton collisions using hard probes. *J. Phys. G* **2017**, *44*, 065001. [CrossRef]

7.　Velasquez, A.O.; Christiansen, P.; Flores, E.C.; Cervantes, I.M.; Paić, G. Color Reconnection and Flowlike Patterns in *pp* Collisions. *Phys. Rev. Lett.* **2013**, *111*, 042001. [CrossRef]

8.　Mishra, A. N.; Paić, G. Did we miss the "melting" of partons in pp collisions? *arXiv* **2019**, arXiv:1905.06918.

9.　Khachatryan, V.; Sirunyan, A.M.; Tumasyan, A.; Adam, W.; Asilar, E.; Bergauer, T.; Brandstetter, J.; Brondolin, E.; Dragicevic, M.; Erö, J.; et al. Studies of inclusive four-jet production with two b-tagged jets in proton-proton collisions at 7 TeV. *Phys. Rev. D* **2016**, *94*, 112005. [CrossRef]

10.　Varga, Z.; Vértesi, R.; Barnaföldi, G.G. Modification of jet structure in high-multiplicity pp collisions due to multiple-parton interactions and observing a multiplicity-independent characteristic jet size. *Adv. High Energy Phys.* **2019**. [CrossRef]

11.　Varga, Z.; Vértesi, R.; Barnaföldi, G.G. Multiplicity Dependence of the Jet Structures in pp Collisions at LHC Energies. *arXiv* **2018**, arXiv:1809.10102.

12.　Sjöstrand, T.; Ask, S.; Christiansen, J.R.; Corke, R.; Desai, N.; Ilten, P.; Mrenna, S.; Prestel, S.; Rasmussen, C.O.; Skands, P.Z. An Introduction to PYTHIA 8.2. *Comput. Phys. Commun.* **2015**, *191*, 159–177. [CrossRef]

13.　Barnaföldi, G.G.; Bíró, G.; Gyulassy, M.; Haranozó, S.M.; Lévai, P.; Ma, G.; Papp, G.; Wang, X.N.; Zhang, B.W. First Results with HIJING++ in High-Energy Heavy-Ion Collisions. *Nucl. Part. Phys. Proc.* **2017**, *373*, 289–290. [CrossRef]

14. Skands, P.; Carrazza, S.; Rojo, J. Tuning PYTHIA 8.1: The Monash 2013 Tune. *Eur. Phys. J. C* **2014**, *74*, 3024. [CrossRef]

15. Ball, R.D.; Bertone, V.; Carrazza, S.; Del Debbio, L.; Forte, S.; Guffanti, A.; Hartland, N.P.; Rojo, J. Parton distributions with QED corrections. *Nucl. Phys. B* **2013**, *877*, 290. [CrossRef]

16. Khachatryan, V.; Sirunyan, A.M.; Tumasyan, A.; Adam, W.; Asilar, E.; Bergauer, T.; Brandstetter, J.; Brondolin, E.; Dragicevic, M.; Erö, J.; et al. Event generator tunes obtained from underlying event and multiparton scattering measurements. *Eur. Phys. J. C* **2016**, *76*, 155. [CrossRef] [PubMed]

17. Buckley, A.; Butterworth, J.; Gieseke, S.; Grellscheid, D.; Höche, S.; Hoeth, H.; Krauss, F.; Lönnblad, L.; Nurse, E.; Richardson, P.; et al. General-purpose event generators for LHC physics. *Phys. Rep.* **2011**, *504*, 145–233. [CrossRef]

18. Pumplin, J.; Stump, D.R.; Huston, J.; Lai, H.L.; Nadolsky, P.M.; Tung, W.K. New generation of parton distributions with uncertainties from global QCD analysis. *J. High Energy Phys.* **2002**, *2002*, 012. [CrossRef]

19. Cacciari, M.; Salam, G.P.; Soyez, G. FastJet user manual. *Eur. Phys. J. C* **2012**, *72*, 1896. [CrossRef]

20. Chatrchyan, S.; Khachatryan, V.; Sirunyan, A.M.; Tumasyan, A.; Adam, W.; Bergauer, T.; Dragicevic, M.; Erö, J.; Fabjan, C.; Friedl, M.; et al. Shape, Transverse Size, and Charged Hadron Multiplicity of Jets in pp Collisions at 7 TeV. *J. High Energy Phys.* **2012**, *2012*, 160. [CrossRef]

21. Ellis, S.D.; Kunszt, Z.; Soper D.E. Large Jets at Hadron Colliders at Order α_s^3: A Look Inside. *Phys. Rev. Lett.* **1992**, *69*, 3615–3618. [CrossRef] [PubMed]

22. Seymour, M.H. Jet Shapes in Hadron Collisions: Higher Orders, Resummation and Hadronization. *Nucl. Phys. B* **1998**, *513*, 269–300. [CrossRef]

23. The ATLAS Collaboration. New ATLAS Event Generator Tunes to 2010 Data. ATL-PHYS-PUB-2011-008, ATL-COM-PHYS-2011-329. Available online: http://inspirehep.net/record/1196773?ln=en (accessed on 27 May 2019).

24. Hoeche, S.; Reichelt, D.; Siegert, F. Momentum conservation and unitarity in parton showers and NLL resummation. *J. High Energy Phys.* **2018**, *2018*, 118. [CrossRef]

25. Cal, P.; Ringer, F.; Waalewijn, W.J. The Jet Shape at NLL'. *arXiv* **2018**, arXiv:1901.06389.

26. Thomas, R.; Kampfer, B.; Soff, G. Gluon Emission of Heavy Quarks: Dead Cone Effect. *Acta Phys. Hung. A* **2005**, *22*, 83–91. [CrossRef]

27. Ortiz, A.; Valencia, P.L. Probing color reconnection with underlying event observables at the LHC energies. *Phys. Rev. D* **2019**, *99*, 034027. [CrossRef]